

# Use of quantitative contrast-enhanced ultrasonography to detect diffuse renal changes in Beagles with iatrogenic hypercortisolism

Hendrik Haers, DVM; Sylvie Daminet, DVM, PhD; Pascale M. Y. Smets, DVM; Luc Duchateau, PhD; Luca Aresu, DVM, PhD; Jimmy H. Saunders, DVM, PhD

**Objective**—To determine the feasibility of quantitative contrast-enhanced ultrasonography (CEUS) for detection of changes in renal blood flow in dogs before and after hydrocortisone administration.

**Animals**—11 Beagles.

**Procedure**—Dogs were randomly assigned to 2 treatment groups: oral administration of hydrocortisone (9.6 mg/kg; n = 6) or a placebo (5; control group) twice a day for 4 months, after which the dose was tapered until treatment cessation at 6 months. Before treatment began and at 1, 4, and 6 months after, CEUS of the left kidney was performed by IV injection of ultrasonography microbubbles. Images were digitized, and time-intensity curves were generated from regions of interest in the renal cortex and medulla. Changes in blood flow were determined as measured via contrast agent (baseline [background] intensity, peak intensity, area under the curve, arrival time of contrast agent, time-to-peak intensity, and speed of contrast agent transport).

**Results**—Significant increases in peak intensity, compared with that in control dogs, were observed in the renal cortex and medulla of hydrocortisone-treated dogs 1 and 4 months after treatment began. Baseline intensity changed similarly. A significant increase from control values was also apparent in area under the curve for the renal cortex 4 months after hydrocortisone treatment began and in the renal medulla 1 and 4 months after treatment began. A significant time effect with typical time course was observed, corresponding with the period during which hydrocortisone was administered. No difference was evident in the other variables between treated and control dogs.

**Conclusions and Clinical Relevance**—Quantitative CEUS allowed detection of differences in certain markers of renal blood flow between dogs treated orally with and without hydrocortisone. Additional studies are needed to investigate the usefulness of quantitative CEUS in the diagnosis of diffuse renal lesions. (*Am J Vet Res* 2013;74:70–77)

Conventional B-mode ultrasonography is a noninvasive imaging technique routinely used in the diagnosis of renal disease that can be used to detect changes in renal size, shape, and parenchymal echogenicity. However, ultrasonographic findings can be unremarkable even when severe renal dysfunction exists. Moreover, an increase in renal echogenicity, as can be observed in patients with renal failure, lacks specificity and sensitivity to be clinically relevant.<sup>1</sup>

Because several diseases influence renal vascular resistance and renal blood flow, quantitative information

Received October 27, 2011.

Accepted April 25, 2012.

From the Departments of Veterinary Medical Imaging and Small Animal Orthopedics (Haers, Saunders), Small Animal Medicine and Clinical Biology (Daminet, Smets), and Physiology and Biometry (Duchateau), Faculty of Veterinary Medicine, Ghent University, 9820 Merelbeke, Belgium; and the Department of Public Health, Comparative Pathology and Veterinary Hygiene, Faculty of Veterinary Medicine, University of Padova, 35020 Agripolis Legnaro PD, Italy (Aresu).

Supported by Esaote-Pie Medical.

Address correspondence to Dr. Haers (hendrikhaers@hotmail.com).

## ABBREVIATIONS

AT	Arrival time
AUC	Area under the curve
BI	Baseline intensity
CEUS	Contrast-enhanced ultrasonography
Cl <sub>creat</sub>	Clearance of exogenous creatinine from plasma
Cl <sub>endo</sub>	Clearance of endo-iohexol from plasma
Cl <sub>exo</sub>	Clearance of exo-iohexol from plasma
GFR	Glomerular filtration rate
PI	Peak intensity
ROI	Region of interest
TTP	Time to peak
uALB	Urinary albumin
ulgG	Urinary immunoglobulin G
W <sub>in</sub>	Wash in
W <sub>out</sub>	Wash out

about renal perfusion can be valuable in the diagnosis of those diseases.<sup>2</sup> Resistive and pulsatility indices can be used with color and spectral Doppler ultrasonography to quantify changes in renal blood flow.<sup>1</sup> However, be-

cause Doppler ultrasonography has low sensitivity for visualizing small arteries and arterioles, an accurate assessment of renal perfusion at the microvascular level is usually not possible with this technique and only large arteries can be assessed.<sup>3</sup>

The limitations of Doppler ultrasonography are overcome by functional hemodynamic imaging modalities such as nuclear scintigraphy, contrast-enhanced CT, or MRI, which are used to evaluate renal perfusion and function in human<sup>4-6</sup> and veterinary medicine.<sup>7-10</sup> However, these methods are not without limitations either, as they can be invasive, result in toxic effects, allow diffusion of tracers, or be influenced by tubular transport or glomerular filtration.<sup>11,12</sup> The aforementioned methods are also more expensive than ultrasonography.

Contrast-enhanced ultrasonography is an imaging modality that promises to improve the diagnostic accuracy of ultrasonography by increasing the intensity of blood-pool echo signals in arteries, veins, and various parenchymal organs through IV injection of ultrasonographic (microbubble) contrast agents.<sup>13</sup> Because microbubble contrast agents remain solely within the vasculature, CEUS improves the detection of perfusion and vascularization in healthy and abnormal organs. In dogs and cats, the liver<sup>14-17</sup> and spleen<sup>18-21</sup> are the parenchymal organs most commonly evaluated with CEUS. Except for certain limitations when used to evaluate splenic tissue, CEUS improves the ability to distinguish between benign and malignant focal parenchymal lesions.

Contrast-enhanced ultrasonography is useful in the assessment of focal renal lesions and renal trauma in humans<sup>22,23</sup> and as a diagnostic aid in veterinary medicine.<sup>24,25</sup> The technique can be used to provide quantitative and qualitative information about renal perfusion.<sup>26-28</sup> Contrast agents used for this purpose are superior to those used in the previously mentioned imaging modalities because they do not diffuse out of the intravascular space yet they are able to pass through all capillary beds because of the tiny diameter of the microbubbles. Moreover, in humans, such contrast agents are regarded as safe and free of hemodynamic effects.<sup>29</sup> The arteriovenous transit time of ultrasonographic contrast agents can be digitally processed, providing time-intensity curves that allow measurement of the rate of agent uptake or clearance in a specific ROI.<sup>30</sup>

In human medicine, quantitative CEUS can be used to detect changes in renal blood flow induced by physiologic and pharmacologic interventions as well as diseases such as renal artery stenosis and chronic allograft nephropathy.<sup>3,11,31-33</sup> In animals with experimentally induced disease, similar uses have been reported.<sup>34,35</sup> In veterinary medicine, reports of quantitative CEUS include those of studies involving healthy kidneys in dogs<sup>36,37</sup> and cats.<sup>38,39</sup>

Hyperadrenocorticism is a disease caused by endogenous overproduction or exogenous long-term use of glucocorticoids.<sup>40</sup> Other than the direct effects of glucocorticoid exposure in mature kidneys on glomerular and tubular function, indirect effects occur through vascular and hemodynamic changes (eg, hypertension) and an increase in cardiac output, total peripheral resistance, and renal blood flow.<sup>41,42</sup> An increase in renal

blood flow attributable to glucocorticoids has been observed in dogs and rats<sup>43-46</sup> but may or may not occur in humans.<sup>47</sup> In a human study<sup>46</sup> of noniatrogenic hyperadrenocorticism, the effects of the disease on renal vascular resistance were investigated through calculation of resistive and pulsatility indices from duplex Doppler images.<sup>46</sup> However, there is a paucity of studies in which CEUS or other functional imaging modalities have been used to evaluate renal blood flow in human and veterinary patients with hyperadrenocorticism. Moreover, to the authors' knowledge, only few reports<sup>48,49</sup> exist in human medicine and none in veterinary medicine involving use of quantitative CEUS in the evaluation of kidneys with diffuse lesions.

The purpose of the study reported here was to determine the feasibility of using quantitative CEUS to detect changes in renal blood flow in dogs before and after oral administration of hydrocortisone. The hypothesis was that quantitative CEUS would aid in the detection of differences in renal blood flow values between dogs treated with and without hydrocortisone, particularly values representing blood volume, with the exception of baseline (background) intensity. If this hypothesis was supported, then this would suggest that quantitative CEUS may have potential as an additional method for diagnosing diffuse renal diseases that affect renal blood flow.

## Materials and Methods

**Animals**—Eleven healthy spayed female research Beagles aged 8.4 to 11 years (median, 10 years), with a body weight ranging from 10.9 to 14.0 kg (median, 12.9 kg), were included in the study. The study was part of a larger investigation of the effect of hydrocortisone administration on renal variables and histologic characteristics. Dogs were judged to be healthy on the basis of their medical history and findings of physical examination, CBC and serum biochemical analysis, abdominal ultrasonography, and 2 consecutive measurements of urinary cortisol-to-creatinine ratio; urine sediment examination, dipstick analysis, specific gravity measurement, protein-to-creatinine ratio determination, and bacterial culture were also performed. The study protocol was approved by the Local Ethical Committee of Ghent University.

**Study design**—Dogs were randomly assigned to 2 treatment groups: 6 Beagles received hydrocortisone<sup>a</sup> (median dose, 9.6 mg/kg, PO, q 12 h), and 5 others (control group) received cellulose-filled gelatin capsules at the same dosing interval. Treatment continued in this manner for 4 months, followed by tapering of the hydrocortisone dose over 1 month (10 mg/kg for 1 week, 5 mg/kg for 2 weeks, and 2.5 mg/kg for 1 week) until no medication was given at 5 months. The study ended at 6 months, which represented 4 weeks after treatment had completely stopped in both groups.

Dogs were monitored for clinical signs suggesting an excess of circulating glucocorticoids, such as polyuria, polydipsia, and polyphagia, and for skin abnormalities (eg, thin skin, hair loss, or comedones). Blood and urine samples were collected from both groups of dogs before treatment began (baseline) and 4 and

6 months after. Furthermore, at the 4- and 6-month points, an ACTH-stimulation test was performed in all dogs from which blood samples were collected and serum was harvested for measurement of cortisol concentrations before and 60 minutes after IM injection of 0.25 mg of synthetic ACTH.<sup>b</sup>

To evaluate renal function, the following variables were measured before and 4 and 6 months after treatment began: serum creatinine and urea concentrations, urinary protein concentration, and GFR as well as urinary concentrations of markers of glomerular function (uALB and uIgG) and tubular function (urinary retinol-binding protein and urinary N-acetyl- $\beta$ -D-glucosaminidase).<sup>50</sup> The urinary concentration of each marker was expressed as a ratio, indexed to the creatinine concentration. Glomerular filtration rate was measured as  $Cl_{creat}$ ,  $Cl_{exo}$ , and  $Cl_{endo}$  on the basis of a protocol reported for cats.<sup>51</sup>

Contrast-enhanced ultrasonography was performed on 4 occasions: before treatment began (time 0) and 1 (time 1), 4 (time 4), and 6 (time 6) months after treatment began. Ultrasonography-guided percutaneous biopsy of the left kidney was performed in each dog approximately 30 minutes after CEUS was performed at times 0, 4, and 6.

**CEUS protocol**—Contrast-enhanced ultrasonography was performed with dogs positioned in dorsal recumbency. Dogs were conscious and held in position by manual restraint. For several dogs, clear identification of the right kidney with a linear transducer was difficult, often resulting in insufficient image quality for further analysis. Therefore, only the left kidney was included in all evaluations. All CEUS examinations were performed with a multifrequency linear array transducer (5 to 7.5 MHz) and a dedicated ultrasonography machine<sup>c</sup> equipped with contrast-specific imaging technology<sup>d</sup> that allowed selective automatic tuning of the contrast agent signal and removal of tissue echoes, enabling selective identification of the microbubbles. The kidneys were scanned continuously in the longitudinal plane during the early arterial and late corticomedullary phases for a total duration of 2 minutes. The mechanical index was set at a low value (0.08 to 0.09) to achieve microbubble resonance with production of harmonic frequencies. Machine settings such as overall gain (61%), time gain compensation, depth (5 cm), persistence, and dynamic range were set at the same values for every examination. Only 1 focal spot was used and was set at the deepest part of the kidney. The transducer was maintained at the same position during CEUS.

An approximately 0.3-mL bolus of contrast medium (sulphur hexafluoride-filled microbubbles<sup>e</sup>)/10 kg of body weight was injected twice IV into a cephalic vein via a 22-gauge indwelling catheter, immediately followed by a 2-mL flush of sterile saline (0.9% NaCl) solution. A 3-way stopcock was used to avoid any delay between injections of contrast agent and saline solution. Imaging was started simultaneously with contrast agent injection. At the end of every bolus injection, the timer was set at 0. In between the contrast agent injections, the microbubbles were destroyed by setting the acoustic power at the highest value and scanning the

kidney, aorta, liver, and spleen for several minutes. This resulted in a decrease in acoustic shadowing artifacts attributable to remnant gas bubbles gathering within the tissues.

**Renal biopsy protocol**—Dogs were sedated with a combination of acepromazine (0.01 mg/kg) and butorphanol (0.01 mg/kg) injected IV. Ten minutes after injection, diazepam (0.2 mg/kg) was administered IV, followed immediately by IV injection of propofol to effect so that endotracheal intubation could be performed. Anesthesia was maintained with 2% isoflurane in oxygen.

All biopsies were performed by an experienced radiologist, as described elsewhere.<sup>52</sup> Large-bore 14-gauge needles<sup>f</sup> (length, 9 cm; specimen notch, 20 mm) were used. Tissue sections from each biopsy sample were prepared with the following stains: H&E, hematoxylin-van Gieson, Martius scarlet blue, periodic acid-Schiff, Masson trichrome, and periodic acid-methenamine silver. Renal tissue slides were evaluated via light microscopy for presence of glomerular, tubular, interstitial, and vascular lesions, and a 4-point scale was used to grade lesion severity (1 = minimal; 2 = mild; 3 = moderate; and 4 = severe). All sections were histologically examined by 3 pathologists who were unaware of dog identity.

**Quantitative analysis**—All CEUS examinations were digitally recorded on a magnetic optic disc as 2-minute video clips, at a rate of 10 frames/s. Clips representing the second injection were imported into specialized computer software<sup>g</sup> for objective quantitative analysis. Two circular ROIs containing

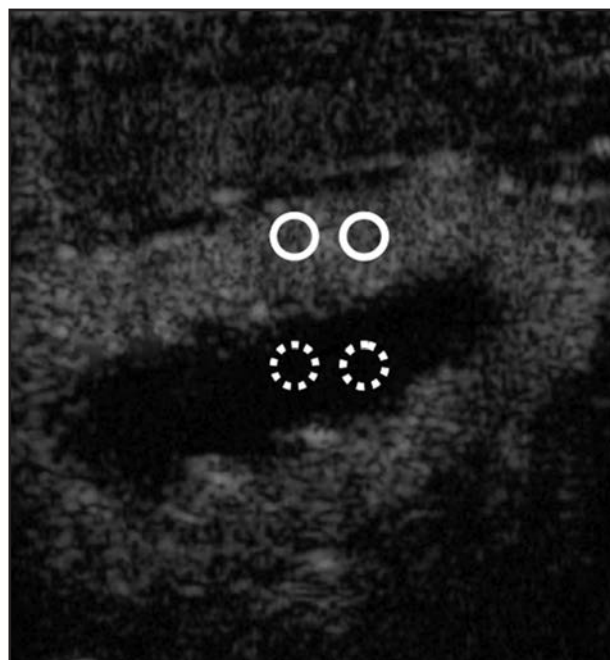


Figure 1—Contrast-enhanced ultrasonographic image of the left kidney of an adult Beagle showing the placement of 2 ROIs manually drawn next to each other in the renal cortex (solid circles) and in the medulla (dashed circles) to measure renal blood flow. Care was taken to avoid blood-filled structures such as arcuate and interlobular arteries within the ROI. The image was obtained 12 seconds after contrast agent injection.

a standardized amount of 712 pixels were manually drawn in the renal cortex, and another 2 were drawn in the medulla (Figure 1). The ROIs were placed at approximately the same location in the renal cortex (parietal aspect nearest to transducer) and medulla (center), with the 2 ROIs in each region being next to each other. Care was taken to avoid blood-filled structures such as arcuate, interlobar, or interlobular arteries within an ROI.

For each ROI, every frame ( $n = 1,200$ ; 10 frames/s) of the complete clip was analyzed as an image stack and resulted in a list of 1,200 mean pixel intensities. The list was saved and imported into a spreadsheet software program.<sup>h</sup> First, the values of the 2 adjacent ROIs of the cortex and medulla for both bolus injections (ie, 4 ROIs) were averaged, resulting in 1 mean pixel intensity value for the cortex and 1 for the medulla. The resulting values were used to create time-intensity curves for the renal cortex and medulla (Figure 2). In a few examinations, respiratory motion resulted in an ROI being located exterior to the renal cortex or medulla. In those situations, the mean pixel intensity values of the frames were deleted and replaced by mean values of adjacent frames.

The time-intensity curves were analyzed for the following blood flow characteristics: BI, averaged for the first 3 seconds after injection; AT, defined as the first point in the curve clearly higher than (within 5 mean pixel intensity values) the mean BI; TTP, defined as the interval from the start of contrast agent injection to the maximum intensity of the curve; PI, corrected for mean BI; AUC, corrected for mean BI, which is proportional to the regional blood volume; and  $W_{in} - W_{out}$ , defined as the increase or decrease in the intensity divided by the time needed for a certain increase or decrease, indicating the speed of bolus transit. Wash in was calculated from data points between 10% higher than the mean BI and 90% of PI. Data points between 90% of PI and the end of the study were used to calculate  $W_{out}$ .

**Statistical analysis**—A computer software program<sup>i</sup> was used to develop a linear mixed model, with assessment point (times 0, 1, 4, and 6), treatment (hydrocortisone vs no hydrocortisone), and their interac-

tion as categorical fixed effects and dog identity as random effect. The  $F$  test was performed to assess the effect of time and treatment on the values of the various renal blood flow variables. Significant differences for single comparisons were defined as values of  $P < 0.05$ . For multiple comparisons, the Bonferroni correction technique was used. Similar analyses were performed to assess the effects of time and treatment on renal function ( $Cl_{creat}$ ,  $Cl_{exo}$ ,  $Cl_{endo}$ , and serum and urinary renal variables).

## Results

**Animals**—All dogs assigned to the hydrocortisone group developed clinical signs of hypercortisolism, such as polyuria, polydipsia, and dermatologic changes as well as increases in serum alkaline phosphatase and alanine aminotransferase activities. Some dogs also developed muscle atrophy and abdominal distention. After 4 months of treatment (time 4), 36 hours after hydrocortisone withdrawal, all dogs in the hydrocortisone group

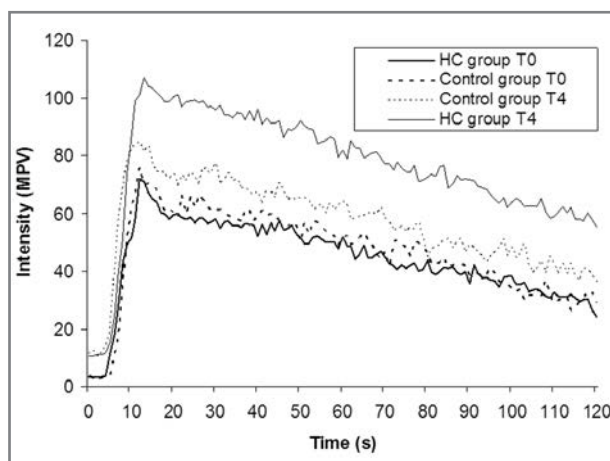


Figure 2—Time-intensity curves showing the mean pixel intensity in the renal cortex before (T0) and after 4 months (T4) of twice-daily hydrocortisone (HC; 9.6 mg/kg, PO;  $n = 6$ ) or placebo (control; 5) administration in adult Beagles. Notice the differences in shape and size of the curves at T0 and T4 (peak of hydrocortisone treatment). MPV = Mean pixel intensity value.

Table 1—Mean  $\pm$  SD values of renal blood flow variables in adult Beagles measured via CEUS before (baseline) and at 1, 4, and 6 months of hydrocortisone (initial dosage, 9.6 mg/kg, q 12 h;  $n = 6$ ) or placebo (5; control group) oral administration.

Variable, by location	Baseline		1 month		4 months		6 months	
	Placebo	Hydrocortisone	Placebo	Hydrocortisone	Placebo	Hydrocortisone	Placebo	Hydrocortisone
<b>Renal cortex</b>								
BI	3.44 $\pm$ 1.17	3.20 $\pm$ 1.16	4.51 $\pm$ 1.24	8.37 $\pm$ 3.74*†	11.07 $\pm$ 2.38†	11.72 $\pm$ 2.67†	5.54 $\pm$ 1.90	4.74 $\pm$ 1.48
PI	76.44 $\pm$ 11.79	71.99 $\pm$ 13.67	73.35 $\pm$ 9.97	94.96 $\pm$ 13.6*†	82.96 $\pm$ 7.42	107.29 $\pm$ 4.77*†	77.51 $\pm$ 9.37	83.19 $\pm$ 7.98
AT	6.63 $\pm$ 1.13	6.94 $\pm$ 2.59	6.34 $\pm$ 1.89	6.68 $\pm$ 1.78	5.40 $\pm$ 1.21	6.33 $\pm$ 1.20	6.47 $\pm$ 0.89	6.38 $\pm$ 1.49
TTP	11.34 $\pm$ 2.37	12.23 $\pm$ 3.69	10.98 $\pm$ 1.19	12.73 $\pm$ 3.86	10.92 $\pm$ 1.47	12.52 $\pm$ 2.65	11.12 $\pm$ 1.36	12.75 $\pm$ 3.00
$W_{in}$	20.75 $\pm$ 5.62	17.73 $\pm$ 5.88	18.14 $\pm$ 5.39	22.26 $\pm$ 6.86	26.38 $\pm$ 6.28	25.56 $\pm$ 4.59†	20.73 $\pm$ 3.59	18.39 $\pm$ 5.91
$W_{out}$	-0.39 $\pm$ 0.05	-0.44 $\pm$ 0.12	-0.37 $\pm$ 0.07	-0.46 $\pm$ 0.09	-0.37 $\pm$ 0.06	-0.43 $\pm$ 0.12	-0.41 $\pm$ 0.05	-0.48 $\pm$ 0.05
AUC	4,812.61 $\pm$ 975.80	4,871.89 $\pm$ 1,278.79	4,406.12 $\pm$ 1,414.31	6,181.31 $\pm$ 1,676.16	5,747.29 $\pm$ 1,054.08*†	7,784.91 $\pm$ 1,213.01	5,200.12 $\pm$ 878.38	5,784.19 $\pm$ 1,315.97
<b>Renal medulla</b>								
BI	2.99 $\pm$ 2.38	3.22 $\pm$ 2.39	4.49 $\pm$ 1.37	7.12 $\pm$ 4.02†	7.91 $\pm$ 2.49†	5.37 $\pm$ 1.42	4.03 $\pm$ 1.70	2.90 $\pm$ 0.62
PI	58.31 $\pm$ 9.65	59.97 $\pm$ 11.35	62.94 $\pm$ 13.67	81.41 $\pm$ 16.80*†	70.29 $\pm$ 5.52	91.81 $\pm$ 7.81*†	67.88 $\pm$ 6.34	71.39 $\pm$ 12.43
AT	13.00 $\pm$ 1.97	13.25 $\pm$ 2.21	11.40 $\pm$ 1.19	13.17 $\pm$ 1.66	10.70 $\pm$ 2.66	11.75 $\pm$ 0.82	13.7 $\pm$ 0.97	11.83 $\pm$ 3.01
TTP	28.4 $\pm$ 2.30	28.00 $\pm$ 1.79	26.8 $\pm$ 1.09	27.5 $\pm$ 1.64	26.8 $\pm$ 1.48	28.83 $\pm$ 1.94	28.6 $\pm$ 2.19	28.67 $\pm$ 1.21
$W_{in}$	4.48 $\pm$ 1.56	4.92 $\pm$ 1.52	4.33 $\pm$ 0.53	5.72 $\pm$ 1.66	4.37 $\pm$ 0.89	5.65 $\pm$ 0.82	4.79 $\pm$ 1.24	4.62 $\pm$ 1.67
$W_{out}$	-0.42 $\pm$ 0.13	-0.47 $\pm$ 0.09	-0.42 $\pm$ 0.16	-0.50 $\pm$ 0.12	-0.44 $\pm$ 0.14	-0.58 $\pm$ 0.09	-0.41 $\pm$ 0.08	-0.56 $\pm$ 0.14
AUC	3,411.34 $\pm$ 947.20	3,669.68 $\pm$ 1,184.29	3,597.55 $\pm$ 1,246.67	5,353.97 $\pm$ 1,417.47*†	4,207.6 $\pm$ 577.52	6,108.62 $\pm$ 931.35*†	4,219.42 $\pm$ 1,130.88	4,670.51 $\pm$ 813.29

\*Value represents a significant ( $P < 0.05$ ) treatment effect. †Value represents a significant ( $P < 0.05$ ) time effect.

failed to respond adequately to ACTH stimulation. At the 6-month assessment point (time 6), 4 weeks after hydrocortisone treatment had been completely withdrawn, clinical signs appeared to have resolved, except for skin changes in some dogs, and clinicopathologic abnormalities were no longer evident. Response to the ACTH stimulation test was within reference limits for all dogs. None of the dogs in the control group developed signs of hypercortisolism or other abnormalities.

**Effects of hydrocortisone administration on renal function**—Hydrocortisone administration resulted in a significant increase in GFR:  $Cl_{creat}$  and  $Cl_{exo}$  were significantly higher in the hydrocortisone group than in the control group at time 4. At all time points, the severity of proteinuria was higher in the control group than in the hydrocortisone group. No significant difference in values of urinary markers was evident between groups. At time 4, proteinuria as well as ratios of uALB to creatinine concentration and uIgG to creatinine concentration were higher than baseline in the hydrocortisone group.

**CEUS of the renal cortex**—Mean  $\pm$  SD values of renal blood flow variables for all treatment-time combinations were summarized (Table 1). A significant ( $P = 0.044$ ) interaction between treatment and time was found for BI. For the same variable, a significant ( $P < 0.001$ ) time effect relative to the value before treatment began (time 0) was identified at times 1 and 4 in the hydrocortisone group. A similar pattern for BI was observed in control dogs; however, a significant ( $P < 0.001$ ) time effect relative to time 0 was evident at time 4. Pairwise comparisons of specific treatment-time combinations revealed a significant ( $P = 0.006$ ) treatment effect at time 1.

In the hydrocortisone group, PI values followed a time course similar to that of the BI values. A significant interaction between treatment and time was detected for PI. A significant time effect relative to time 0 was identified at time 1 ( $P < 0.001$ ) and time 4 ( $P < 0.001$ ). Pairwise comparisons of specific treatment-time combinations revealed a significant ( $P = 0.001$  and  $P < 0.001$ , respectively) treatment effect at the same time points.

For  $W_{in}$  of contrast agent, a significant ( $P = 0.010$ ) time effect was found at time 4 for the treated dogs, with significantly higher values at that point than at times 0 or 6. The pattern for AUC values was similar to that of BI values in treated dogs, with a significant ( $P < 0.001$ ) difference between time 0 and time 4 and a significant ( $P = 0.010$ ) difference between the hydrocortisone and control groups at time 4. No significant differences were identified among values for AT, TTP, or  $W_{out}$ .

**CEUS of the renal medulla**—Baseline contrast agent intensity in the medulla in treated dogs had a pattern different from that in the cortex. Values increased and reached a maximum at time 1, with gradual decrease toward time 4 and additional decrease at time 6, at which point values were slightly lower than at time 6. A significant ( $P = 0.006$ ) time effect was observed for time 1, compared with time 0, with values at time 1 being higher. The BI in the control dogs had a pattern similar to that in the cortex, with a significant ( $P = 0.002$ ) time effect. No treatment effect was evident.

On the other hand, the PI in treated dogs had a pattern similar to that in the renal cortex, with the same significant time effects between times 1 and 0 ( $P < 0.001$ ) and times 4 and 0 ( $P < 0.001$ ). Significant treatment effects were identified at time 1 ( $P = 0.012$ ) and time 4 ( $P = 0.004$ ), as were observed in the cortex.

The AUC values in treated dogs were similar in pattern to those in the renal cortex. A significant time effect was evident at time 1 ( $P < 0.001$ ) and time 4 ( $P < 0.001$ ), compared with at time 0. Pairwise differences of specific treatment-time combinations revealed significant treatment effects at time 1 ( $P = 0.013$ ) and time 4 ( $P = 0.008$ ). No significant differences were identified among values for AT, TTP,  $W_{in}$ , or  $W_{out}$ .

**Renal biopsy specimens**—No significant vascular changes were identified in any of the biopsy specimens. However, glomerular, tubular, and interstitial lesions were observed. Already at time 0, mild to moderate diffuse and global glomerulosclerosis was detected (4/6 treated dogs and 3/5 control dogs). Minimal to mild interstitial inflammation (2/6 treated dogs and 5/5 control dogs) and fibrosis (2/5 control dogs) were identified.

Glomerulosclerosis was more pronounced in both dog groups at time 4 than at time 0. Specimens from control dogs had evidence of progression of the preexisting glomerulosclerotic lesions noted at time 0. Three treated dogs that did not have interstitial inflammation at time 0 developed minimal to mild interstitial inflammation and fibrosis. In all 5 control dogs, interstitial inflammation remained at time 4, progressing in severity in 4 dogs.

By time 6, glomerulosclerosis was evident in all dogs, with increasing percentages of obsolescent glomeruli. Interstitial inflammation and fibrosis persisted in control dogs, and scores persisted or increased in treated dogs by time 6.

## Discussion

In the present study, quantitative CEUS of the renal cortex and medulla in healthy Beagles revealed significant differences in values of blood flow variables between those treated with and without hydrocortisone for a prolonged period (9.6 mg/kg, PO, q 12 h for 4 months, followed by a tapering dosage for 1 month).

The renal blood flow variables measured can be grouped into those representing blood volume (PI and AUC) and those representing blood flow velocity (AT, TTP,  $W_{in}$ , and  $W_{out}$ ). The hydrocortisone-induced increase detected in our study in PI and AUC can be likely explained by the effect of glucocorticoids on renal vascularity and hemodynamics, subsequently leading to an increase in GFR. The GFR increase at time 4 was confirmed by the significant increase in  $Cl_{creat}$  and  $Cl_{exo}$ , more severe proteinuria, uALB-to-creatinine concentration ratio, uIgG-to-creatinine concentration ratio, and urinary retinol-binding protein-to-creatinine concentration ratio in the hydrocortisone group, compared with in the control group.

Species-specific differences in the mechanism of glucocorticoid-induced changes in renal blood flow and GFR exist.<sup>40</sup> With the exception of systemic effects such as hypertension, plasma volume expansion

(mineralocorticoid effects), and changes in vascular tone, glucocorticoid administration in dogs reportedly causes a significant increase in renal blood flow, accompanied by a decrease in renal vascular resistance.<sup>45,46</sup> Moreover, catabolic effects of glucocorticoids lead to increases in plasma amino acid concentrations, leading to an increase in renal blood flow and GFR due to renal vasodilation.<sup>43</sup> Our results indicated that quantitative CEUS was able to reveal an increase in renal blood volume values, suggesting the combined effect of glucocorticoids (decrease in renal vascular resistance, renal vasodilation, and plasma volume expansion) on renal hemodynamics.

A limitation of the present study was that no correlation could be made between CEUS and biopsy results, as histologic evaluation of biopsy specimens revealed no significant vascular changes. Additionally, the potential influence of consecutive renal biopsies on our results needs to be considered. At the 4-month CEUS evaluation, only 1 biopsy had been performed previously, whereas by the time of the 6-month evaluation, 2 biopsies had been performed. Because ROIs were established in approximately the same location as the biopsies, these biopsies could potentially have affected renal blood flow values. In a study<sup>53</sup> of the effect of percutaneous renal biopsy on the appearance of contrast harmonic ultrasonographic images, biopsy-associated lesions resolved 2 to 3 weeks after the biopsies had been performed and there was no effect of hydrocortisone administration on healing. In that study, however, only the morphological effect on renal vasculature and healing was assessed, and no quantification of contrast agent was performed. Therefore, an effect on renal blood flow variables could not be fully excluded. It would be less likely that, had lesions resolved 2 to 3 weeks after biopsy, a significant influence on renal blood flow values would remain 4 and 2 months after biopsy, at times 4 and 6, respectively. Moreover, because the same standardized procedure was used for all biopsies in all dogs, any biopsy effect should have been no different between treated and control dogs. Therefore, absolute values in both groups could be different but treatment effect would not be influenced, although theoretically, the time effect could be impacted. One might expect a larger influence (increase) of renal blood flow at time 6 than at time 4 because 2 biopsies were performed prior to CEUS at time 6; however, that did not happen. Additionally, it would be unlikely that results for the renal medulla and cortex would be similar when biopsies were only obtained from the cortex.

In fluid dynamics, the Bernoulli principle states that for an inviscid flow, an increase in the speed of the fluid occurs simultaneously with a decrease in pressure or a decrease in the fluid's potential energy.<sup>54</sup> Theoretically, as a consequence of this principle and of GFR maintenance as an important function of kidneys, an increase in renal blood volume and hence, pressure, results in a decrease in blood flow velocity in the afferent arterial vessels.<sup>54</sup> In the present study, however, none of the blood flow velocity values differed significantly between hydrocortisone-treated and control dogs. One possible cause might be the previously reported decrease in renal vascular resistance that occurs with an

increase in the volume of circulating glucocorticoids in dogs.<sup>45,46</sup> Glomerular filtration rate is determined by intraglomerular pressure, which is controlled by vasoconstriction of afferent or efferent arterioles. As shown in rats, nitrous oxide-mediated vasodilation of these pre- and postglomerular arterioles results in an increase in renal blood flow and GFR.<sup>44</sup> This decrease in resistance possibly neutralizes the increase in blood pressure that results from larger blood volume, leading to unhampered blood flow from efferent to afferent arterioles, with no noticeable change in velocity.

When blood flow results for the renal medulla were compared with those of the cortex in the present study, similarities in significant time and treatment effects between the 2 became apparent. These similarities were reasonable given that the renal medulla does not receive blood directly from a main artery but is supplied by 10% to 15% of efferent arterioles from the cortex.<sup>55</sup> Consequently, changes in medullary blood flow depend on changes in cortical flow.<sup>55</sup> Lower PI amplitudes and greater blood flow velocities were evident in the medulla versus the cortex after hydrocortisone treatment. Renal vascular anatomy provides an explanation for this difference in perfusion.<sup>56</sup> Once blood enters the renal medulla, it has already passed the renal artery, several arterial branches, pre- and postglomerular arterioles, and glomerular capillaries located in the cortex. Therefore, contrast agent reaches the medulla at a later stage, resulting in an increase in AT and TTP values. The decrease in PI is attributable to the less extensive capillary network in the medulla versus the cortex. Moreover, as contrast agent passes the cortex, a portion of the microbubbles are destroyed before entering the medulla.

One remarkable result of our study was the significantly higher values of BI at times 1 and 4 in the cortex of treated dogs, and at time 1 in the medulla, compared with in other regions. The BI represented the ultrasonographic intensity of renal tissue averaged over a period of 3 seconds after injection of contrast agent, before its arrival in the renal cortex. No significant change in BI values was expected. However, approximately similar significant changes as observed for blood volume (vs blood flow) variables were present, with increasing values in the renal cortex of hydrocortisone-treated dogs at times 1 and 4 and at time 1 in the medulla. A significant treatment effect was also observed at time 1 in renal cortical tissue, with a time course similar to that of the blood volume variables. Surprisingly, a significant increase in BI values was also observed at time 4 in the renal cortex and medulla of control dogs, with again similar time course. Possible explanations include erroneous machine settings or systematic technical error at certain time points or an increase in renal echogenicity. Technical errors were unlikely to have influenced the findings because standardized settings were used, the same CEUS procedure was performed by the same sonographer, and one would expect erroneous settings to result in nondifferential misclassification of values between the cortex and medulla or between treatment groups.

An increase in renal echogenicity would most likely explain the differences in BI. In hepatic tissue, an increase in circulating glucocorticoids results in gly-

cogen deposition, which leads to an increase in liver echogenicity.<sup>57</sup> The same does not occur in kidneys. Another possibility is the influence of repeated biopsies on renal echogenicity; however, as a standardized biopsy procedure was used, this option is an unlikely explanation. When biopsy specimens were examined, differences in interstitial fibrosis and diffuse and global glomerulosclerosis in both treated and control dogs were observed. At time 0 (before hydrocortisone administration), minimal to mild interstitial fibrosis and mild to moderate glomerulosclerosis were already evident in several dogs, which might have been attributable to the age of the dogs.<sup>58,59</sup> When findings at time 4 were compared with those at time 0, glomerulosclerosis was more pronounced in both treatment groups and 2 additional treated dogs developed minimal to mild fibrosis. By time 6, all dogs had developed glomerulosclerosis, interstitial fibrosis persisted in control dogs, and lesion severity appeared to have increased in treated dogs. One possible explanation for the increased severity is the acceleration of age-related changes in the treated group by hydrocortisone administration.

Because histologic changes also worsened in the control group with time, another explanation could be progression of preexisting renal lesions. Fibrotic and sclerotic lesions increase the echogenicity of parenchymal organs and could therefore explain the observed differences in BI at time 4 in both treatment groups. However, because histologic lesions were worse at time 4, this might suggest that BI should have been higher at this time point, and yet, the opposite was found.

Another reason for the progressive histologic changes during the 6-month study period is cavitation of ultrasonography contrast agents. This occurs at high acoustic power when microbubbles burst, which results in adjacent tissues including capillaries being damaged by the released energy.<sup>60</sup> However, because a low mechanical index was used in our study, we are unable to make any definitive conclusions regarding the significant changes in BI.

Another remarkable finding was that  $W_{in}$  (an indicator of blood flow velocity) was influenced by time in the renal cortex of treated dogs, with higher values at time 4 than at time 0. No effect of treatment was present for this variable. Hence, the steep slope of the time-intensity curve indicating higher inflow of renal blood was present at this time point in treated dogs, when hydrocortisone administration was at its maximum, but also in control dogs. Biopsy specimens from both treated and control dogs had evidence of increased interstitial inflammation at time 4 versus 0, which could be a possible explanation for the increase in  $W_{in}$ . However, interstitial inflammation was more severe at time 6, whereas  $W_{in}$  values were lower. These observed changes cannot be explained.

Although only left kidneys were investigated in the present study, results suggested that quantitative CEUS can be used to detect changes in certain renal blood flow variables in dogs undergoing hydrocortisone treatment, which is presumed to have affected renal hemodynamics. Because of this, quantitative CEUS could have potential in the discrimination among healthy renal tissue and benign or malignant causes of hyper-

echoic kidneys. Additional studies are warranted to assess the diagnostic value of quantitative CEUS in dogs with diffuse renal disease.

- 
- a. Hydrocortisone USP, Paddock Laboratories Inc., Minneapolis, Minn.
  - b. Synacthen, Novartis Pharma, Vilvoorde, Belgium.
  - c. MyLab 30 CV, Esaote, Genoa, Italy.
  - d. Contrast Tuned Imaging (CnTI), Esaote, Genoa, Italy.
  - e. Sonovue, Bracco Diagnostics Inc, Milan, Italy.
  - f. Vet-Core, Surgivet, Dublin, Ohio.
  - g. ImageJ, US National Institutes of Health, Bethesda, Md.
  - h. Microsoft Excel, Office 2003, Microsoft Corp, Redmond, Wash.
  - i. SAS, version 9.2, SAS Institute Inc, Cary, NC.
- 

## References

1. Tublin ME, Bude RO, Platt JF. The resistive index in renal sonography: where do we stand? *AJR Am J Roentgenol* 2003;180:885–892.
2. Regan MC, Young LS, Geraghty J, et al. Regional renal blood flow in normal and disease states. *Urol Res* 1995;23:1–10.
3. Wei K, Le E, Bin J-P, et al. Quantification of renal blood flow with contrast-enhanced ultrasound. *J Am Coll Cardiol* 2001;37:1135–1140.
4. Read S, Allen C, Hare C. Applications of computed tomography in renal imaging. *Nephron Clin Pract* 2006;103:c29–c36.
5. Choyke PL, Kobayashi H. Functional magnetic resonance imaging of the kidney using macromolecular contrast agents. *Abdom Imaging* 2006;31:224–231.
6. Haufe SE, Riedmuller K, Haberkorn U. Nuclear medicine procedures for the diagnosis of acute and chronic renal failure. *Nephron Clin Pract* 2006;103:c77–c84.
7. Mitchell SK, Toal RL, Daniel GB, et al. Evaluation of renal hemodynamics in awake and isoflurane-anesthetized cats with pulsed-wave Doppler and quantitative renal scintigraphy. *Vet Radiol Ultrasound* 1998;39:451–458.
8. Aumann S, Schoenberg SO, Just A, et al. Quantification of renal perfusion using an intravascular contrast agent (part 1): results in a canine model. *Magn Reson Med* 2003;49:276–287.
9. Bouma JL, Aronson LR, Keith DG, et al. Use of computed tomography renal angiography for screening feline renal transplant donors. *Vet Radiol Ultrasound* 2003;44:636–641.
10. O'Dell-Anderson KJ, Twardock R, Grimm JB, et al. Determination of glomerular filtration rate in dogs using contrast-enhanced computed tomography. *Vet Radiol Ultrasound* 2006;47:127–135.
11. Kalantarinia K, Okusa MD. Ultrasound contrast agents in the study of kidney function in health and disease. *Drug Discov Today Dis Mech* 2007;4:153–158.
12. Young LS, Regan MC, Barry MK, et al. Methods of renal blood flow measurement. *Urol Res* 1996;24:149–160.
13. Haers H, Saunders JH. Review of clinical characteristics and applications of contrast-enhanced ultrasonography in dogs. *J Am Vet Med Assoc* 2009;234:460–470.
14. Ziegler LE, O'Brien RT, Waller KR, et al. Quantitative contrast harmonic ultrasound imaging of normal canine liver. *Vet Radiol Ultrasound* 2003;44:451–454.
15. O'Brien RT, Iani M, Matheson J, et al. Contrast harmonic ultrasound of spontaneous liver nodules in 32 dogs. *Vet Radiol Ultrasound* 2004;45:547–553.
16. Kanemoto H, Ohno K, Nakashima K, et al. Characterization of canine focal liver lesions with contrast-enhanced ultrasound using a novel contrast agent—Sonazoid. *Vet Radiol Ultrasound* 2009;50:188–194.
17. Nakamura K, Takagi S, Sasaki N, et al. Contrast-enhanced ultrasonography for characterization of canine focal liver lesions. *Vet Radiol Ultrasound* 2010;51:79–85.
18. Ohlerth S, Dennler M, Rüeffli E, et al. Contrast harmonic imaging characterization of canine splenic lesions. *J Vet Intern Med* 2008;22:1095–1102.
19. Rossi F, Leone VF, Vignoli M, et al. Use of contrast-enhanced ultrasound for characterization of focal splenic lesions. *Vet Radiol Ultrasound* 2008;49:154–164.
20. Ivancic M, Long F, Seiler G. Contrast harmonic ultrasonography

- of splenic masses and associated liver nodules in dogs. *J Am Vet Med Assoc* 2009;234:88–94.
21. Taeymans O, Penninck D. Contrast enhanced sonographic assessment of feeding vessels as a discriminator between malignant vs. benign focal splenic lesions. *Vet Radiol Ultrasound* 2011;52:457–461.
  22. Siracusano S, Quaia E, Bertolotto M, et al. The application of ultrasound contrast agents in the characterization of renal tumors. *World J Urol* 2004;22:316–322.
  23. Regine G, Atzori M, Miele V, et al. Second-generation sonographic contrast agents in the evaluation of renal trauma. *Radiol Med* 2007;112:581–587.
  24. Haers H, Vignoli M, Paes G, et al. Contrast harmonic ultrasonographic appearance of focal space-occupying renal lesions. *Vet Radiol Ultrasound* 2010;51:516–522.
  25. Haers H, Pey P, Smets P, et al. Contrast harmonic ultrasound appearance of consecutive percutaneous renal biopsies in dogs. *Vet Radiol Ultrasound* 2011;52:640–647.
  26. Taylor GA, Ecklund K, Dunning PS. Renal cortical perfusion in rabbits: visualisation with color amplitude imaging and an experimental microbubble-based US contrast agent. *Radiology* 1996;201:125–129.
  27. Abildgaard A, Klow NE, Jakobsen JE, et al. Effect of ultrasound contrast medium in color Doppler and power Doppler visualisation of blood flow in canine kidneys. *Acta Radiol* 1997;38:445–453.
  28. Cosgrove D. Angiogenesis imaging—ultrasound. *Br J Radiol* 2003;76:S43–S49.
  29. Kalantarinia K. Novel imaging techniques in acute kidney injury. *Curr Drug Targets* 2009;10:1184–1189.
  30. Schmid V, Lang J. Intravascular ultrasound contrast media. *Vet Radiol Ultrasound* 1995;36:307–314.
  31. Kishimoto N, Mori Y, Nishiue T, et al. Renal blood flow measurement with contrast-enhanced harmonic ultrasonography: evaluation of dopamine-induced changes in renal cortical perfusion in humans. *Clin Nephrol* 2003;59:423–428.
  32. Fischer T, Filimonow S, Dieckhofer J, et al. Improved diagnosis of early kidney allograft dysfunction by ultrasound with echo enhancer—a new method for the diagnosis of renal perfusion. *Nephrol Dial Transplant* 2006;21:2921–2929.
  33. Schwenger V, Korosoglou G, Hinkel U-P, et al. Real-time contrast-enhanced sonography of renal transplant recipients predicts chronic allograft nephropathy. *Am J Transplant* 2006;6:609–615.
  34. Pollard RE, Dayton PA, Watson KD, et al. Motion corrected Candence CPS ultrasound for quantifying response to vasoactive drugs in a rat kidney model. *Urology* 2009;74:675–681.
  35. Claudon M, Barnewold CE, Taylor GA, et al. Renal blood flow in pigs: changes depicted with contrast-enhanced harmonic US imaging during acute urinary obstruction. *Radiology* 1999;212:725–731.
  36. Bahr A, Wrigley R, Salman M. Quantitative evaluation of Imagent as an abdominal ultrasound contrast medium in dogs. *Vet Radiol Ultrasound* 2000;41:50–55.
  37. Waller KR, O'Brien RT, Zagzebski JA. Quantitative contrast ultrasound analysis of renal perfusion in normal dogs. *Vet Radiol Ultrasound* 2007;48:373–377.
  38. Kinns J, Aronson L, Hauptman J, et al. Contrast-enhanced ultrasound of the feline kidney. *Vet Radiol Ultrasound* 2010;51:168–172.
  39. Leinonen MR, Raekallio MR, Vainio OM, et al. The effect of the sample size and location on contrast ultrasound measurement of perfusion parameters. *Vet Radiol Ultrasound* 2011;52:82–87.
  40. Smets P, Meyer E, Maddens B, et al. Cushing's syndrome, glucocorticoids and the kidney. *Gen Comp Endocrinol* 2010;169:1–10.
  41. Mangos GJ, Whitworth JA, Williamson PM, et al. Glucocorticoids and the kidney. *Nephrology* 2003;8:267–273.
  42. Walker BR. Glucocorticoids and cardiovascular disease. *Eur J Endocrinol* 2007;157:545–559.
  43. Hall JE, Morse CL, Smith MJ, et al. Control of arterial pressure and renal function during glucocorticoid excess in dogs. *Hypertension* 1980;2:139–148.
  44. Denton KM, Li M, Anderson WP, et al. Glomerular hypertension and hyperfiltration in adrenocorticotropic-induced hypertension in rats: the role of nitric oxide. *J Hypertens* 2001;19:327–334.
  45. Kubota E, Hayashi K, Matsuda H, et al. Role of intrarenal angiotensin II in glucocorticoid-induced renal vasodilation. *Clin Exp Nephrol* 2001;5:186–192.
  46. Novellas R, de Gopegui RR, Espada Y. Determination of renal vascular resistance in dogs with diabetes mellitus and hyperadrenocorticism. *Vet Rec* 2008;163:592–596.
  47. Connell JMC, Whitworth JA, Davies DL, et al. Hemodynamic, hormonal and renal effects of adrenocorticotropic hormone in sodium-restricted man. *J Hypertens* 1988;6:17–23.
  48. Hosotani Y, Takahashi N, Kiyomoto H, et al. A new method for evaluation of split renal cortical blood flow with contrast echography. *Hypertens Res* 2002;25:77–83.
  49. Tsuruoka K, Yasuda T, Koitabashi K, et al. Evaluation of renal microcirculation by contrast-enhanced ultrasound with Sono-zoid as a contrast agent. *Int Heart J* 2010;51:176–182.
  50. Smets PMY, Lefebvre HP, Aresu L, et al. Renal function and morphology in aged Beagle dogs before and after hydrocortisone administration. *PLoS ONE* 2012;7:e31702.
  51. van Hoek I, Vandermeulen E, Duchateau L, et al. Comparison and reproducibility of plasma clearance of exogenous creatinine, exo-iohexol, endo-iohexol, and Cr-51-EDTA in young adult and aged healthy cats. *J Vet Intern Med* 2007;21:950–958.
  52. Vaden SL. Renal biopsy of dogs and cats. *Clin Tech Small Anim Pract* 2005;20:11–22.
  53. Haers H, Smets P, Pey P, et al. Contrast harmonic ultrasound appearance of consecutive percutaneous renal biopsies in dogs. *Vet Radiol Ultrasound* 2011;52:640–647.
  54. Badeer HS. Hemodynamics for medical students. *Adv Physiol Educ* 2001;25:44–52.
  55. Kalantarinia K, Belcik JT, Patrie JT, et al. Real-time measurement of renal blood flow in healthy subjects using contrast-enhanced ultrasound. *Am J Physiol Renal Physiol* 2009;297:1129–1134.
  56. Christensen GC. The urogenital apparatus. In: Evans HE, Christensen GC, eds. *Miller's anatomy of the dog*. Philadelphia: WB Saunders Co, 1979;544–554.
  57. Nyland TG, Mattoon JS, Herrgesell EJ. Liver—diffuse liver disease. In: Nyland TG, Mattoon JS, eds. *Small animal ultrasound*. 2nd ed. Philadelphia: WB Saunders Co, 2002;108–113.
  58. Pomeroy MJ, Robertson JL. The relationship of age, sex, and glomerular location to the development of spontaneous lesions in the canine kidney: analysis of a life-span study. *Toxicol Pathol* 2004;32:237–242.
  59. Heiene R, Kristiansen V, Teige J, et al. Renal histomorphology in dogs with pyometra and control dogs, and long term clinical outcome with respect to signs of kidney disease. *Acta Vet Scand* 2007;49:13.
  60. Stride EP, Coussios CC. Cavitation and contrast: the use of bubbles in ultrasound imaging and therapy. *Proc Inst Mech Eng H* 2010;224:171–191.